# NMR Relaxivities of Paramagnetic, Ultra-High Spin Heterometallic Clusters within Polyoxometalate Matrix as a Function of Solvent and Metal Ion

Nicolas Schork,[a] Masooma Ibrahim,[b] Ananya Baksi,[c] Steffen Krämer,[d] Annie K. Powell,[b, e, f] and Gisela Guthausen*[a]

Selectivity and image contrast are always challenging in magnetic resonance imaging (MRI), which are – inter alia – addressed by contrast agents. These compounds still need to be improved, and their relaxation properties, i.e., their paramagnetic relaxation enhancement (PRE), needs to be understood. The main goal is to improve specificity and relaxivities, especially at the high magnetic fields currently exploited not only in material science but also in the medical environment. Longitudinal and transverse relaxivities, $r_1$ and $r_2$, which correspond to the longitudinal and transverse relaxation rates $R_1$ and $R_2$, normalized to the concentration of the paramagnetic moieties, need to be considered because both contribute to the image contrast. $^1$H-relaxivities $r_1$ and $r_2$ of high-spin hetero-metallic clusters were studied containing lanthanide and transition-metal ions within a polyoxometalate matrix. A wide range of magnetic fields from 0.5 T/20 MHz to 33 T/1.4 GHz was applied. The questions addressed here concern the rotational and diffusion correlation times which determine the relaxivities and are affected by the solvent's viscosity. Moreover, the variation of the lanthanide and transition-metal ions of the clusters provided insights into the sensitivity of PRE with respect to the electron spin properties of the paramagnetic centers as well as cooperative effects between lanthanides and transition metal ions.

## Introduction

Nuclear magnetic resonance (NMR) and especially magnetic resonance imaging (MRI) often involve paramagnetic systems. Whether in form of (super-)paramagnetic particles, ions in solution, aggregates, nanogels or as paramagnetic clusters or molecules, the paramagnetism and the time-scales of hyperfine fluctuations determine the mechanisms and in consequence the application area.[1–6] Basically, at least one unpaired electron spin is required, and the hyperfine fields of the studied nuclei and the unpaired electron spin needs to fluctuate – crudely with frequencies in the kHz range (transverse relaxation $R_2$) and the Larmor frequency ranges (longitudinal relaxation $R_1$). The

NMR signals of the observed nuclei thus are sensitive to static as well as to fluctuating hyperfine couplings between the nuclear spin $I$ and the electronic spin $S$. Static hyperfine interactions lead to shifts of the NMR lines. Thus, the NMR "chemical" shift range is significantly expanded, e.g. in the case of $^1$H up to 100 ppm instead of the usual 12 ppm. Fluctuating hyperfine interactions cause an additional relaxation path leading to the enhancement of $R_1$ and $R_2$ nuclear spin relaxation rates of the observed, hyperfine coupled nuclear spins. This mechanism is known as paramagnetic relaxation enhancement (PRE).[5,7–11]

Early descriptions of PRE were made by Solomon (dipolar coupled spin pairs), Bloembergen, Morgan (PRE) and others, for example [12–14]. It is already clear at these early days of NMR that detailed knowledge about correlation times, distances, coordination and molecular geometry, and conformation are essential for choosing the correct description of PRE.

Gadolinium (III) ions (Gd$^{III}$) are commonly used and preferred as paramagnetic centers for contrast agents especially at low magnetic fields due to their high number of unpaired electron spins, their high symmetry and isotropy, their high magnetic moment, and their long electron spin relaxation times.[5,6,15] However, their use in biology, especially in organisms is still questionable due to toxicity. For the typically applied contrast agents, the relaxivities tend to decrease with magnetic field,[4–6,16] which is an additional argument for research on new contrast agents, which are based on alternative paramagnetic species, e.g. Dy$^{III}$.[2,3,11,17–19]

Other examples are the heterometallic high-spin coordination clusters [Fe$_{10}$Ln$_{10}$(Me-tea)$_{10}$(Me-teaH)$_{10}$(NO$_3$)$_{10}$] with the lanthanides (Ln) Y$^{III}$, Gd$^{III}$, Tb$^{III}$, Dy$^{III}$, Er$^{III}$, and Tm$^{III}$, abbreviated as

[a] Dr. N. Schork, Prof. Dr. G. Guthausen
Karlsruhe Institute of Technology (KIT), Institutes of Mechanical Engineering and Mechanics and of Water Chemistry and Technology, Adenauerring 20b, 76131 Karlsruhe, Germany
E-mail: Gisela.Guthausen@kit.edu
[b] Dr. M. Ibrahim, Prof. Dr. A. K. Powell
Karlsruhe Institute of Technology (KIT), Institute of Nanotechnology (INT), Hermann-von-Helmholtz-Platz 1, 76344 Eggenstein-Leopoldshafen, Germany
[c] Dr. A. Baksi
Technische Universität Dortmund, Anorganische Chemie, Otto-Hahn-Straße 6, 44227 Dortmund, Germany
[d] Dr. S. Krämer
CNRS, LNCMI-EMFL, Université Grenoble Alpes, INSA T, and UPS, Boîte Postale 166, 38042, Grenoble Cedex 9, France
[e] Prof. Dr. A. K. Powell
Karlsruhe Institute of Technology (KIT), Institute of Inorganic Chemistry, Engesserstrasse 15, 76131 Karlsruhe, Germany
[f] Prof. Dr. A. K. Powell
Karlsruhe Institute of Technology (KIT), Institute for Quantum Materials and Technologies (IQMT), Hermann-von-Helmholtz-Platz 1, 76344 Eggenstein-Leopoldshafen, Germany

{Fe₁₀Ln₁₀}.[5,6,20,21] Polyoxometalate (POM) clusters were used as host assemblies for contrast agents.[22,23] We explored [Ln₃₀Co₈Ge₁₂W₁₀₈O₄₀₈(OH)₄₂(OH₂)₃₀]⁵⁶⁻ abbreviated as {Ln₃₀Co₈}, these POMs were also studied with Ln∈[Gd<sup>III</sup>, Dy<sup>III</sup>, Eu<sup>III</sup>, Y<sup>III</sup>].[24] The main solvent was water as a 10:90 H₂O:D₂O mix. The use of D₂O is due to NMR radiation damping at high magnetic fields. The water relaxivities determined by PRE of {Fe₁₀Ln₁₀} and {Ln₃₀Co₈} clusters were measured over a very wide range of ¹H Larmor frequencies also above 1 GHz, which is reported only in[25] apart from the own work. The alteration of the lanthanide (Ln) metal ions (at structurally similar sites within the same scaffold) in {Fe₁₀Ln₁₀} and {Ln₃₀Co₈} made it possible to differentiate the impacts of electronic states and molecular dynamics on PRE. In all cases the transverse relaxivity $r_2$ was found to increase with magnetic field in contrast to the more complex behavior of $r_1$ as a function of the magnetic field.

In the present study, we further address questions about the diverse correlation times entering the equations of PRE[5,6] on a qualitative level. By varying the solvent, mainly the time scales of diffusion and rotational fluctuations of the hyperfine interactions are influenced, but not the electronic properties of the POMs. Additionally, the Mn<sup>II</sup> and Zn<sup>II</sup> analogues in the {Ln₃₀M₈} scaffolds were studied, which allows conclusions about cooperative effects between Gd<sup>III</sup> and Co<sup>II</sup>, Mn<sup>II</sup>, Zn<sup>II</sup> ions in a given cluster apart from the separation of contributions of the Gd<sup>III</sup>/Dy<sup>III</sup> ions and the other metal ions to the relaxivities of the solvent molecules. The experimental results are discussed within a simplified description of PRE.

## Structure of the Polyoxometalate-Based Heterometallic Clusters

Recently, we reported about the synthesis of a new class of polyoxometalate (POM)-based hybrid structures {Ln₃₀M₈},[26,27] where Ln∈[Gd, Dy] and M∈[Zn, Mn, Co]. Diverse analytical techniques have been used to study the polyoxometalates {Ln₃₀M₈}, including single-crystal X-ray diffraction to measure the atoms present in the anionic moiety, differential thermal analysis (DTA)/thermogravimetric analysis (TG) to obtain the number of attached water molecules, and inductively coupled plasma-mass spectrometry (ICP-MS) for elemental analysis studies, i.e. the atomic percentages present in the compound. Using all these techniques the accurate sum formula and molecular weights were determined.

- Cs₁₄Co<sup>II</sup>₆Na₃₀[{(GeW₉O₃₄)₂Dy<sup>III</sup>₃(μ₂-OH)₃(H₂O)}₆{Co<sup>II</sup>₂Dy<sup>III</sup>₃-(μ₃-OH)₆(OH₂)₆}₄]·370H₂O {**Dy₃₀Co₈**}, 43426 g/mol
- Cs₂Co<sup>II</sup>₆Na₄₂[{(GeW₉O₃₄)₂Gd<sup>III</sup>₃(μ₂-OH)₃(OH₂)₃}₆{Co<sup>II</sup>₂Gd<sup>III</sup>₃(μ₃-OH)₆(OH₂)₆}₄]·340H₂O {**Gd₃₀Co₈**}, 41680 g/mol
- CsMn<sup>II</sup>₆Na₃₇[{(GeW₉O₃₄)₂Gd<sup>III</sup>₃(CO₃)(OH₂)}₆{Mn<sup>II</sup>₂Gd<sup>III</sup>₃(μ₃-OH)₆(OH₂)₆}₄]·295H₂O {**Gd₃₀Mn₈**}, 40564 g/mol
- CsZn<sup>II</sup>₂Na₄₅[{(GeW₉O₃₄)₂Gd<sup>III</sup>₃(CO₃)(OH₂)}₆{Zn<sup>II</sup>₂Gd<sup>III</sup>₃(μ₃-OH)₆(OH₂)₆}]·295H₂O {**Gd₃₀Zn₈**}, 40633 g/mol

All these POMs exhibit a common hollow cage structure comprised of four {Ln<sup>III</sup>₃M<sup>II</sup>₂(OH₂)₆} clusters as nodes and six {(GeW₉O₃₄)₂Ln<sup>III</sup>₃(OH₂)} units as linkers forming the giant tetrahe-

dron (Figure 1). In the linker unit one of the lanthanide centers has one exchangeable water molecule, whereas there are three exchangeable water molecules attached to the 3d metal ions (Figure 1a, b). This new class of purely inorganic materials allow the variation of paramagnetic ions in a diamagnetic POM matrix that causes significant changes in the magnetic behavior of the clusters. Thus, {Ln₃₀M₈} can not only offer model systems for testing theories related to magnetic properties and PRE, but also provide new materials for highly specific and novel applications.[26,27]

## PRE in a Nutshell: Principle and Influencing Parameters

A common attempt to quantitatively describe PRE is based on the separation of effects which will be described very crudely in the following. First, inner and outer sphere contributions are differentiated – depending on the distance between a paramagnetic center and the observed nucleus as well as on the time scales of the fluctuations. Second, the hyperfine interaction itself is split into Curie and dipolar terms. The notation used in this paper is that of ref. [11]. Well knowing that the description is even more simplified here, nevertheless, the experimental findings can be matched to the equations and allow an estimate of the important factors and therefore are a guide to understand the observations. We focus on the longitudinal relaxation:

Inner sphere: The inner sphere longitudinal PRE $R_{1,is}$ is given by

$$R_{1,is} = fq\frac{1}{T_{1M} + \tau_M}, \tag{1}$$

where $f$ is the ratio of concentrations of the paramagnetic compound and the solvent, $q$ is the number of water molecules in the first coordination sphere, $\tau_M$ is the residence time of the water molecules, and $R_{1M} = 1/T_{1M}$ is the relaxation rate of the nuclei in that first coordination sphere. This term in eq. 1 is the sum of dipolar ($R_{1,is,DD}$) and Curie ($R_{1,is,C}$) contributions described in eq. 2 and eq. 4.
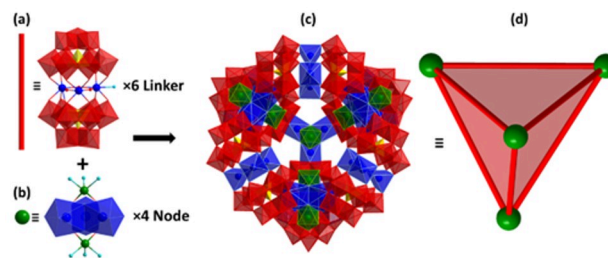


**Figure 1.** Combined polyhedral/ball and stick representation of Ln₃₀M₈. (a) {Ln<sup>III</sup>₃} core in sandwich-type building block linker {(GeW₉O₃₄)₂Ln<sup>III</sup>₃(OH)}. (b) Heterometallic node {Ln<sup>III</sup>₃M<sup>II</sup>₂(OH₂)₆}. (c) Giant tetrahedral architecture Ln₃₀M₈. (c) The giant tetrahedral architecture in Ln₃₀M₈ is formed by connection of the six linker units via four heterometallic node units. Polyhedral color scheme: WO₆: red, GeO₄: yellow, MO₆: green, LnOₙ: blue. Color scheme for balls: Ln: blue, O: red, aqua ligand: turquoise, and M: green.

The dipolar contribution $R_{1, is, DD}$ to PRE is given in that picture by:

$$R_{1, is, DD} \propto \gamma_I^2 \mu_B^2 g_j^2 \, J(J+1) \frac{1}{r^6} [3 \, J(\omega_I, \, \tau_C) + 7 \, J(\omega_S, \, \tau_C)] \qquad (2)$$

$\gamma_I$ is the nuclear gyromagnetic ratio, $\mu_B$ the Bohr magneton, $g_j$ the Landé factor, while $J$ represents the total electronic spin quantum number. $r$ is very essential and describes the distance between the observed nucleus and the paramagnetic species. In addition to the squared dipolar part of the hyperfine interaction (the factors before the square bracket), the fluctuations are modeled in terms of the spectral densities $J(\omega, \, \tau_C)$ described by Lorentzian functions (eq. 3):

$$J(\omega_I, \, \tau_C) = \frac{\tau_C}{1 + \omega_I^2 \tau_C^2}, \; J(\omega_S, \, \tau_C) = \frac{\tau_C}{1 + \omega_S^2 \tau_C^2}. \qquad (3)$$

The nuclear and electronic Larmor frequencies $\omega_{I,S}$ at a given magnetic field $B_0$ and the correlation time $\tau_C$, which is given by the rotational and exchange correlation times as well as the electronic relaxation, thereby determine the spectral densities.

Additionally, the Curie term has to be considered

$$R_{1, is, C} \propto \gamma_I^2 B_0^2 \, \mu_B^4 g_j^4 \, J^2(J+1)^2 \frac{1}{r^6} \frac{1}{(3k_B T)^2} \, 3 \, J(\omega_I, \, \tau_{CC}) \qquad (4)$$

with the spectral density

$$J(\omega_I, \, \tau_{CC}) = \frac{\tau_{CC}}{1 + \omega_I^2 \tau_{CC}^2}, \qquad (5)$$

where $\tau_{CC}$ is the Curie correlation time in eq. 5. Here, the thermal energy $k_B T$ has to be considered ($k_B$: Boltzmann constant, $T$: absolute temperature), in addition to the pronounced magnetic field dependence.

Outer sphere: Again, dipolar and Curie terms contribute, the equations for the longitudinal relaxation are also taken from.[11] The dipolar term is given by the properties of nuclear and electronic spins. In addition, the relative diffusion $D$ and the closest distance $a$ determine the diffusional correlation time (eq. 6)

$$\tau_D = \frac{a^2}{D}. \qquad (6)$$

The Avogadro number $N_A$ and the molar concentration $[C]$ are also present in the equations (eq. 7 and eq. 8). In addition, the time-averaged electronic spin ("Curie spin") $S_C$ needs to be considered.

$$R_{1, os, DD} \propto \frac{\gamma_I^2 \mu_B^2 g_j^2 \, N_A[C]}{aD}$$
$$\left[ 6 \left( J(J+1) \quad S_C \coth\left(\frac{B_0 \mu_B g_j}{2k_B T}\right) \quad S_C^2 \right) J(\omega_I, \, \tau_S, \, \tau_D) \right. \qquad (7)$$
$$\left. + 7 \, S_C \coth\left(\frac{B_0 \mu_B g_j}{2k_B T}\right) J(\omega_S, \, \tau_S, \, \tau_D) \right]$$

The Curie contribution in the outer sphere reads as:

$$R_{1, os, C} \propto \frac{\gamma_I^2 \mu_B^2 g_j^2 \, N_A[C]}{aD} \, S_C^2 \, J^A(\omega_I, \, \tau_D) \qquad (8)$$

These equations (eq. 7 and eq. 8) were applied to model the longitudinal $^1$H relaxivities $r_1$ as a function of $^1$H Larmor frequency for Dy(DTPA):[2,11] Curie contributions were shown to dominate at Larmor frequencies $> 400$ MHz for inner sphere, $> 700$ MHz for outer sphere contributions. The transverse relaxivities follow similar dependencies apart from the fact that $r_2$ is more sensitive to fluctuations with frequencies in the kHz range compared to MHz to GHz for $r_1$. For further detail we refer to reference [11]. A comprehensive study of Ln$^{III}$-DOTA complexes was published, which uses an extension of this model. In particular the impact of the orbital angular momentum of Ln is discussed.[28]

## Results and Discussion

### Factors Influencing PRE

PRE induced by the studied paramagnetic metal clusters can thus be interpreted in terms of hyperfine relaxation, which depends not only on the properties of the paramagnetic ions, but also on distances and relative dynamics of the solvent molecules with respect to the paramagnetic cluster. The solvent molecules in the vicinity of the paramagnetic metal ions therefore show a different relaxation behavior, which usually enhances both longitudinal and transverse relaxation, because an additional relaxation path is introduced by the fluctuating hyperfine interactions. PRE thus depends on the structure and electronic properties of the paramagnetic clusters as well as on the molecular dynamics.[5,29] As stated, important factors are the coordination number $q$, the rotational and diffusion correlation times, the residence time distribution of solvent molecules near the paramagnetic centers (exchangeable moieties), and the properties of the paramagnetic metal ions, e.g., their effective magnetic moments and their electron spin relaxation times.

More complex paramagnetic systems require investigations concerning the diverse correlation times in the equations for PRE.[5,6] Time scales of diffusion and rotational correlation times of the fluctuating hyperfine interactions can be altered via the viscosity of the solvent. In the present case of complex POMs, cooperative effects of the paramagnetic species also need to be discussed since several Ln and M ions are present. Additionally, the Co$^{II}$, Mn$^{II}$ and Zn$^{II}$ analogues in the {Gd$_{30}$M$_8$} scaffolds were

studied. This allows conclusions regarding cooperative effects between $Gd^{III}$ and $Co^{II}$, $Mn^{II}$, $Zn^{II}$ ions in a given cluster to be drawn. Furthermore, the $Zn^{II}$ analogue allows the separation of contributions of the $Gd^{III}/Dy^{III}$ ions and the transition-metal ions to the relaxivities of the solvent molecules to be gauged. Thus, in the present paper, questions about the molecular dynamics are addressed as well as the question about the cooperativity of the paramagnetic ions in the cluster.

## PRE of $\{Ln_{30}Co_8\}$ ($Ln \in [Gd^{III}, Dy^{III}]$) in Water and Glycerine Mixtures

In an earlier study, $\{Fe_{10}Ln_{10}\}$ and $\{Ln_{30}Co_8\}$ clusters were measured in water and propanediol to get some insight into the impact of solvent properties on PRE, especially on the rotational, exchange and diffusion correlation times.[24] This approach was further explored by investigating PRE of $\{Dy_{30}Co_8\}$ and $\{Gd_{30}Co_8\}$ in mixtures of water (90% $D_2O$, 10% $H_2O$, abbreviated as D in the following) and the more viscous glycerine (propane-1,2,3-triol, $C_3H_8O_3$, abbreviated as G) in the volume ratios 50:50 and 20:80. Data were already published for 100:0, which are used here for comparison and further interpretation of PRE in these solvent mixtures.[24]

Relaxivities for $\{Dy_{30}Co_8\}$ in various mixtures are summarized in Figure 2 on a logarithmic scale. PRE of $\{Dy_{30}Co_8\}$ in water shows a significant increase of longitudinal relaxivity $r_1$ as a function of Larmor frequency by a factor of 10 and an even stronger increase of transverse relaxivities $r_2$ by a rough factor of 100. A flattening of the dispersion is observed above 800 MHz for both relaxivities. While $r_1$ leads to a positive MRI contrast, which is the more desired effect, $r_2$ leads in most MRI experiments to a diminished magnetic resonance (MR) intensity which is usually less desirable.

The relaxivity measurements provide evidence (Figure 2) that a concentration quantification of the paramagnetic species in MR images necessarily requires the knowledge of the correlation times of the molecules experiencing PRE (evident also in eq. 3,5,6): When changing the solvent composition towards larger viscosities, $r_1$ decreases over the measured range of Larmor frequencies and becomes approximately frequency independent at about 5 times lower $r_1$ value (D:G 20:80) while $r_2$ shows a pronounced increase with viscosity and as a function of Larmor frequency (please note the logarithmic scale). Viscosity is thereby related to rotational and diffusion correlation times of the solvent molecules, which directly enter the PRE equations (eq. 1–8). In other words, the effect is more pronounced at higher magnetic fields and lower viscosities. Overall, the behavior of $\{Dy_{30}Co_8\}$ resembles what is observed for (super-)paramagnetic particles.[30,31]

Similar observations were made for $\{Gd_{30}Co_8\}$, although the electronic properties of the paramagnetic ions are significantly different (Figure 3): While $Dy^{III}$ has non-zero angular momentum and typically short electron relaxation times ($10^{-13}$ s), $Gd^{III}$ has no orbital angular momentum and usually long electron relaxation times ($10^{-7}$ s).[32] Therefore, the various terms in the presented simplified PRE model are expected to be consider-
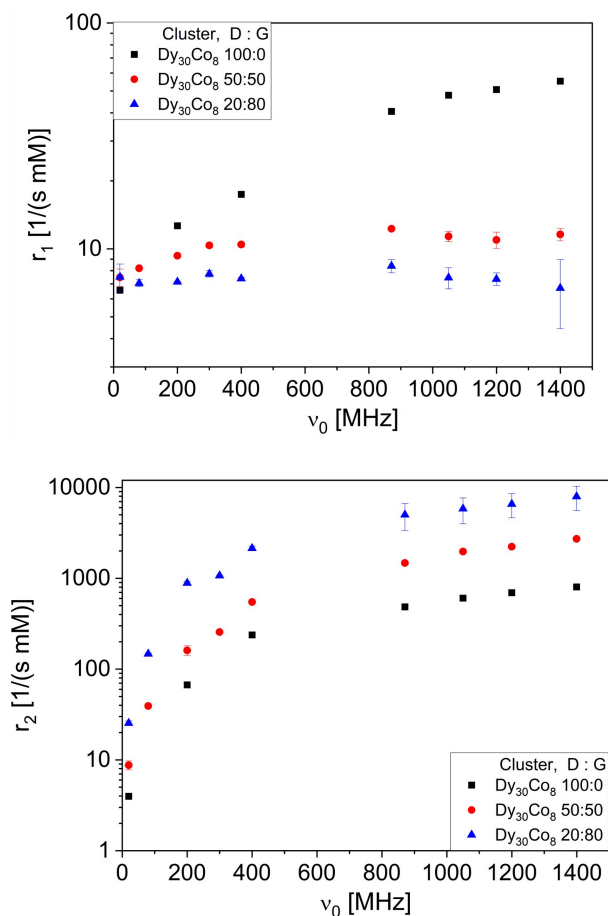


**Figure 2.** Dispersion of longitudinal (top) and transverse (bottom) relaxivities $r_1$ and $r_2$ of $\{Dy_{30}Co_8\}$ solutions in water (D)/glycerine (G) mixtures. While the electronic properties of the cluster are constant, the fluctuation spectrum of the hyperfine interaction between solvent molecules and paramagnetic centers changes upon varying the viscosity of the solvent, which is reflected in the relaxation dispersions.

ably different. $\{Gd_{30}Co_8\}$ exhibits larger $r_1$, and its dispersion shows a decrease with magnetic field when compared with the Dy analogue. The dispersion of $r_1$ becomes more pronounced in the case of D:G mixtures for $\{Gd_{30}Co_8\}$. Namely, at Larmor frequencies $< 200$ MHz, $r_1$ becomes larger with increased glycerine concentration while $r_1$ steeply decreases with Larmor frequency leveling off to similar $r_1$ values as $r_1(\{Dy_{30}Co_8\})$. These findings give hints on the importance of the interplay of the diverse influencing factors when aiming at modeling PRE and finding an optimal contrast agent for a given purpose.

In comparison to $\{Dy_{30}Co_8\}$, the transverse relaxivity $r_2$ in $\{Gd_{30}Co_8\}$ is less field-dependent, particularly for the purely aqueous system. In the case of D:G mixtures, $r_2$ increases at Larmor frequencies [20, 350] MHz, while the field dependence gets more pronounced at high viscosities and shows similar trends at lower values when compared to PRE of the $\{Dy_{30}Co_8\}$ cluster.

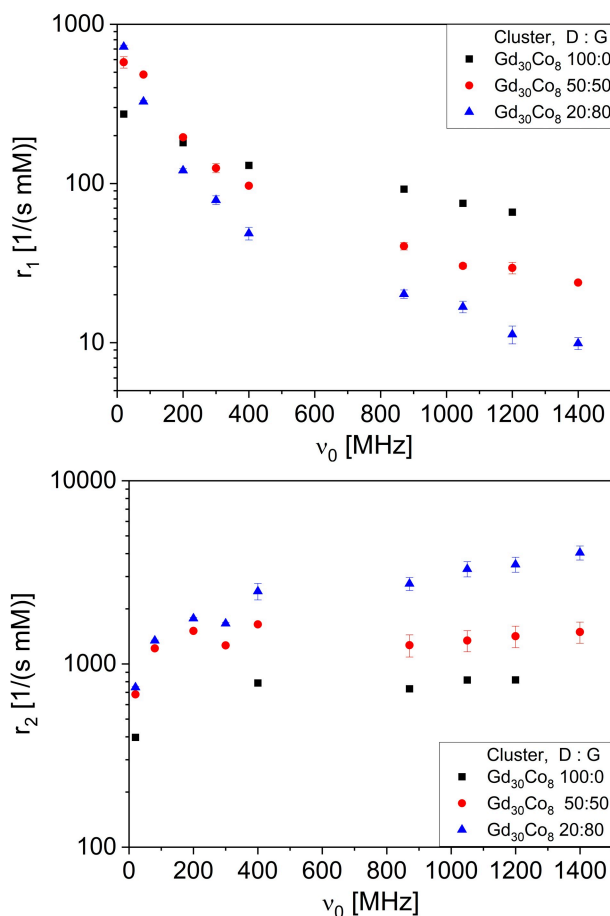**Figure 4.** Longitudinal relaxivities of the $Gd_{30}M_8$ compounds with $M \in [Mn^{II}, Co^{II}, Zn^{II}]$ in the three different solvent mixtures as a function of Larmor frequency The lines are guides to the eye. The impact of the 3d metal ions is clearly seen in the comparison of three solvent mixtures.



**Figure 3.** Relaxivities of $Gd_{30}Co_8$ solutions in water (D)/glycerin (G) mixtures. The long electronic correlation times of the $Gd^{III}$ ions lead to changes in relaxivity dispersions of $r_1$ and $r_2$, which are obscured by the diffusion and rotational correlation times of solvents with higher viscosity.

## Longitudinal Relaxivity $r_1$ of {$Gd_{30}M_8$} ($M \in [Mn^{II}, Co^{II}, Zn^{II}]$)

In {$Gd_{30}M_8$}, not only the Ln ions can be paramagnetic, but also the 3d metal ions. The question arises whether 4f and 3d orbitals couple, and whether cooperative effects are also observed in PRE. As not only the electronic properties influence the relaxivities, the three solvent compositions were also measured for the analogue {$Gd_{30}M_8$} with paramagnetic Mn ions, while for the diamagnetic Zn the aqueous solution was studied. Additionally, in these samples the trend of decreasing $r_1$ as a function of Larmor frequency (Figure 4) is found, but with a different dependence.

Focusing first on the aqueous solution study, the change from $Co^{II}$ to $Mn^{II}$ to $Zn^{II}$ results in a larger longitudinal PRE at low Larmor frequencies. At Larmor frequencies from 200 MHz, the $Mn^{II}$-analogue provides the largest $r_1$, whereas $r_1$ of the $Co^{II}$ and $Zn^{II}$ clusters coincide within experimental error. At low frequencies < 200 MHz, all three compounds show different $r_1$.

Similar observations were made for the two other solvent compositions. {$Gd_{30}Co_8$} shows stronger dependencies on the magnetic field with increasing viscosity. The longitudinal
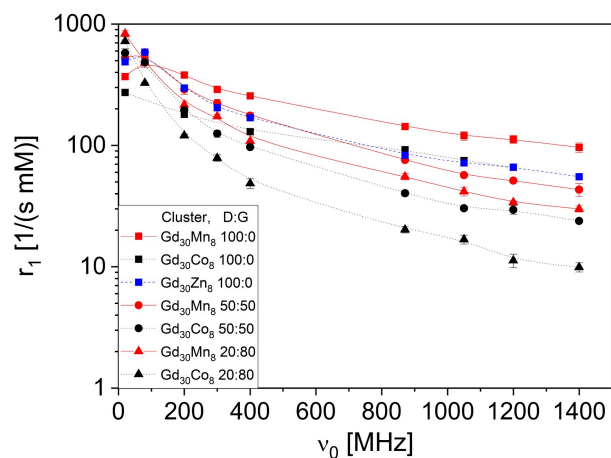
relaxivities of {$Gd_{30}Mn_8$} show a similar trend, although at lower frequencies an emerging maximum appears with increasing viscosity. Depending on the 3d metal ion and on the solvent's correlation times, different hyperfine relaxation mechanisms contribute to $r_1$ to different extents resulting in a different weighting (eq. 1–8). This leads to field and solvent dependent longitudinal relaxivities.

As mentioned, the $r_1$ values at high magnetic fields are in the same order of magnitude for clusters containing magnetic $Co^{II}$ and non-magnetic $Zn^{II}$ and differ for the $Mn^{II}$ cluster. This is of particular interest, since the rotational and diffusional correlation times are almost constant in this situation. The dispersion curves thus reveal the contribution of the electronic properties to PRE. Investigations of the magnetocaloric effect (MCE) revealed entropic changes for $Zn_8$ of 10.4 J/kg/K; for $Co_8$ of 10.7 J/kg/K and for $Mn_8$ of 14.0 J/kg/K. These measurements of the MCE allowed conclusions on the effect of the $M^{II}$ ion to be drawn.[27] {$Gd_{30}Co_8$} can be understood within the picture of 30 non-interacting $Gd^{III}$ ions and 8 $Co^{II}$ ions in the cluster, although antiferromagnetic couplings or small anisotropy cannot completely be neglected. On the other hand, PRE of $Co^{II}$ ions is usually described by typical longitudinal electronic relaxation times $T_{1e} \in [3, 6]*10^{-12}$ s, using $g = 2$ and $S = 3/2$. These values are not necessarily valid in the present case.[5]

The corresponding findings for {$Gd_{30}Zn_8$} are similar concerning the interpretation of the MCE, using the concept of 30 $Gd^{III}$ ions with small antiferromagnetic couplings in the Gd-triangles (Figure 1). $Zn^{II}$ is diamagnetic and therefore does not contribute to PRE, which is therefore determined by the $Gd^{III}$ ions with $g = 2$ and $S = 7/2$.

The finding that $r_1$ of {$Gd_{30}Zn_8$} and {$Gd_{30}Co_8$} coincide in water therefore sheds some light on the role of the $M^{II}$ ions on PRE. In the case of $Co^{II}$, their contribution to PRE is almost negligible compared to the impact of $Gd^{III}$.

Additionally, the properties of {$Gd_{30}Mn_8$} are in line with this picture. $Mn^{II}$ ions are paramagnetic and therefore contribute to

PRE with typical values $g = 2$, $S = 5/2$, and $T_{1e}$ in the order of $3*10^{11}$ s, which is an order of magnitude larger compared to typical values for $Co^{II}$. This difference in electronic properties of the single ions and electronic interactions in the compound could therefore explain why there is a significant contribution from the $Mn^{II}$ ions to PRE of $\{Gd_{30}Mn_8\}$. Interestingly, this contribution seems insignificant for $\{Gd_{30}Co_8\}$.

**Transverse Relaxivity $r_2$ of $\{Gd_{30}M_8\}$ (M$\in$[$Mn^{II}$, $Co^{II}$, $Zn^{II}$])**

Similar to the case for $r_1$, the transverse relaxivities $r_2$ (Figure 5) depend on Larmor frequency, the viscosity of the solvent and, in addition, on the impact of the 3d metal ions. In principle, small $r_2$ are preferred, which is observed for the $\{Gd_{30}Co_8\}$ cluster in water. The general trend is an increase of $r_2$ with Larmor frequency, while the slope is more pronounced below 200 MHz and for the solutions with higher viscosity. In contrast: In pure water, $r_2$ is almost constant above 200 MHz within experimental error, while the increase is most pronounced for 20:80 D:G, irrespective of the 3d metal ion.

Similar arguments as for the longitudinal relaxivities hold for a phenomenological interpretation of these data: Taking the parameters and findings described above into account, the transverse PRE may be interpreted as that of a nanoparticle in suspensions of different viscosity, which determines rotational and diffusion correlation times in the commonly used PRE descriptions. The similarity between $\{Gd_{30}Mn_8\}$ and $\{Gd_{30}Co_8\}$ compared to $\{Gd_{30}Zn_8\}$ regarding the dependence of $r_2$ on the Larmor frequency at $\nu_0 > 80$ MHz allows us to draw the conclusion that the $M^{II}$ ions paramagnetic properties are decisive. An increase of $r_2$ is observed for all viscosities for $\{Gd_{30}Mn_8\}$ and $\{Gd_{30}Co_8\}$ while $r_2$ of $\{Gd_{30}Zn_8\}$ in water initially is constant but starts to decrease at larger fields.



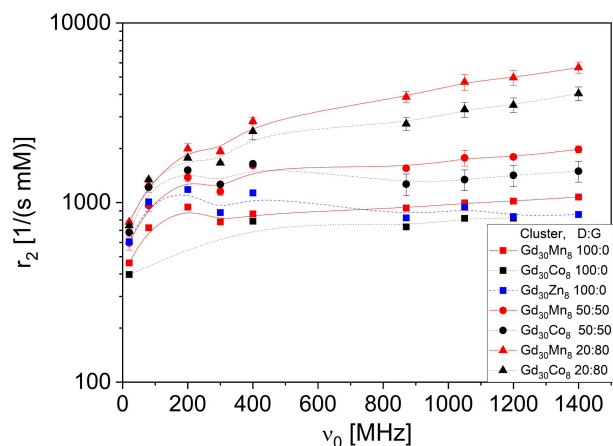**Figure 5.** Transverse relaxivities $r_2$ of the $Gd_{30}M_8$ compounds with M$\in$[$Mn^{II}$, $Co^{II}$, $Zn^{II}$] in the three different solvent mixtures as a function of Larmor frequency. The lines are guides to the eye. The impact of the 3d metal ions is clearly seen leading to different field dependencies and absolute values of $r_2$.

## Conclusions

$^1$H relaxivities $r_1$ and $r_2$ were measured on solutions of $Ln_{30}M_8$ in water/glycerine (D/G) mixtures to reveal the impact of the solvent's composition as well as the nature of Ln and M ions on paramagnetic relaxation enhancement (PRE) of $\{Ln_{30}M_8\}$. The $r_1$ and $r_2$ values indicate the effectiveness of these MRI contrast agents. The variation of the lanthanide and transition-metal ions of the clusters provides insights into the sensitivity of PRE with respect to the electron spin properties of the paramagnetic centers as well as cooperative effects between lanthanides and transition metal ions. $Dy^{III}$ has short electronic relaxation times, which is reflected in the field dependencies of PRE in water, especially when compared to the $Gd^{III}$ analogues also in water. The importance of the electronic relaxation is evident in all investigated solvent compositions as it is reflected in the different field dependence especially for $r_1$. These findings are consistent with properties of other contrast agents and could further be proven by low field NMR relaxivities, EPR or NMRD on heteronuclei with small gyromagnetic ratio.

An interesting aspect is to gauge the effect of solvent viscosity on the longitudinal and transverse relaxivities, $r_1$ and $r_2$, in this study by using water and glycerin mixtures. Both, longitudinal and transverse relaxivities were found to depend on composition and magnetic field. The effect of solvent's viscosity on the relaxivities is found enhanced at highest fields and low viscosities. Moreover, at highest frequencies the longitudinal and transverse dispersions flatten for all compounds, irrespective of the solvent's viscosity and the metal ion. These findings indicate the importance of rotational and diffusion correlation times, which modulate the hyperfine interactions leading to PRE.

An additional aspect concerning the composition of the clusters is the choice of the rare earth metal ion. Not only the magnetism of the 3d ions – whether dia- or paramagnetic – influences PRE, but also the electronic properties and the overlap of the atomic orbitals with the 4f ions. Further work is devoted to simulations of PRE for obtaining the contributions of hyperfine relaxation quantitatively.

## Experimental Section

### Synthesis

- $Cs_{14}Co_6Na_{30}[\{(GeW_9O_{34})_2Dy^{III}_3(\mu_2\text{-}OH)_3(H_2O)\}_6\{Co^{II}_2Dy^{III}_3\text{-}(\mu_3\text{-}OH)_6(OH_2)_6\}_4] \cdot 370 H_2O$ $\{Dy_{30}Co_8\}$[26]
- $Cs_2Co^{II}_6Na_{42}[\{(GeW_9O_{34})_2Gd^{III}_3(\mu\text{-}OH)_3(OH_2)_3\}_6\{Co^{II}_2Gd^{III}_3(\mu_3\text{-}OH)_6(OH_2)_6\}_4] \cdot 340 H_2O$ $\{Gd_{30}Co_8\}$
- $CsMn^{II}_6Na_{37}[\{(GeW_9O_{34})_2Gd^{III}_3(CO_3)(OH_2)\}_6\{Mn^{II}_2Gd^{III}_3(\mu_3\text{-}OH)_6(OH_2)_6\}_4] \cdot 295 H_2O$ $\{Gd_{30}Mn_8\}$
- $CsZn_2Na_{45}[\{(GeW_9O_{34})_2Gd^{III}_3(CO_3)(OH_2)\}_6\{Zn_2Gd^{III}_3(\mu_3\text{-}OH)_6(OH_2)_6\}_4] \cdot 295 H_2O$ $\{Gd_{30}Zn_8\}$[27]

were synthesized according to the published methods and were characterized by IR spectroscopy.[24,26,27] All reactions were carried out under aerobic conditions. All other reagents were purchased commercially and were used without further purification.

For the current studies, {Ln$_{30}$M$_8$} were dissolved in 90% D$_2$O/10% H$_2$O (Supplier: Deutero, Germany). Five dilutions were prepared: 0, 0.2, 0.4, 0.6, 0.8 and 1 mM as PRE of these clusters is rather large and is expected to linearly depend on the concentration of the paramagnetic moieties. As Lanthanides, Gd and Dy were investigated, while M was either Co, Mn, or Zn. The investigated clusters were easily soluble in water. Clear colored aqueous solutions were formed during preparation. The pH value of the solutions is neutral. Even after more than a year of storage no change was observed and the dispersions are therefore regarded as stable, even more as the relaxivities do not change. Additionally, the solvent was modified: Instead of water, mixtures of water (at 20 °C: viscosity η ≈ 1,002 g/(m s)) and glycerin (propane-1,2,3-triol, C$_3$H$_8$O$_3$; at 20 °C: viscosity η ≈ 1,76 kg/(m s), density ρ ≈ 1.263–1.265 g/cm$^3$; supplier: Carl Roth GmbH, Germany) were used in order to modify the correlation times of rotational and diffusion degrees of freedom: the volume ratios of glycerin to water were 80:20, 50:50, and 0:100, while water was 10% H$_2$O, 90% D$_2$O. As stated, care was taken that the investigated samples were homogeneous dispersions without separation and sediments. Apart from the optical inspection, the mono-exponential relaxation behavior and the linearity of the relaxation rates versus the concentration were reliable indicators (see below).

## Mass Spectrometry

Solution and gas phase stability of the polyoxometalate-based heterometallic clusters were studied using high resolution electrospray ionization mass spectrometry (HRESI-MS). A few cluster crystals of {Dy$_{30}$Co$_8$}, {Gd$_{30}$Co$_8$}, {Gd$_{30}$Mn$_8$}, and {Gd$_{30}$Zn$_8$} were dissolved in 50:50 (v/v) H$_2$O:ACN and were electrosprayed into a Waters' Synapt G2S mass spectrometer and analyzed in the negative ion mode. Subsequent to the analysis in the negative ion mode, all clusters were found intact with varying number of counter cations and water molecules (Figure 6). For {Dy$_{30}$Co$_8$}, charge envelopes with charge states ranging from 17- to 11- were observed, and the peaks can be assigned as Na$_{13-19}$ [Cs$_{14}$Co$^{II}_6$[{(GeW$_9$O$_{34}$)$_2$Dy$^{III}_3$(μ$_2$-OH)}(H$_2$O)}$_6${Co$^{II}$Dy$^{III}_3$-(μ$_3$-OH)$_6$ (OH$_2$)$_6$}$_4$]·(H$_2$O)$_x$]$^{17\ 11}$ (x ∈ [50,200]). For example, the peak at m/z 2389 is assigned to [Cs$_{14}$Na$_{14}${Dy$_{30}$Co$_8$}(H$_2$O)$_{124\pm50}$]$^{16}$. All peaks are broad due to the varying H$_2$O loss. The number of H$_2$O molecules vary from ∼70-175 as derived from the peak width. Similarly, ∼60–175, ∼70–210 and ∼100–230 H$_2$O molecules were observed for 17-, 15- and 14- fold charge states, respectively. Charge states of 17- to 10- were observed for {Gd$_{30}$M$_8$} (M ∈ [Mn$^{II}$, Co$^{II}$, Zn$^{II}$]). In general all peaks can easily be assigned. {Gd$_{30}$Mn$_8$} is assigned as Na$_{20-27}$ [CsMn$^{II}_6$[{(GeW$_9$O$_{34}$)$_2$Gd$^{III}_3$(CO$_3$)(OH$_2$)}$_6$ {Mn$^{II}_2$Gd$^{III}_3$(μ$_3$-OH)$_6$(OH$_2$)$_6$}$_4$]·(H$_2$O)$_x$]$^{17\ 10}$ ([CsNa$_{20-27}$ {Gd$_{30}$Mn$_8$}(H$_2$O)$_x$]$^{17\ 10}$) (Figure 6). The clusters remained intact even under ESI-MS conditions and in presence of high voltage (2–3 kV).

## $^1$H – Frequencies 870–1400 MHz

High-field NMR relaxivity studies were performed at the Laboratoire National des Champs Magnétiques Intenses (LNCMI) in Grenoble equipped with 24 MW resistive magnet providing variable fields up to 37 T in a 34 mm room temperature bore. As resistive magnets provide access to variable fields (field ramp rate of 5 T/min), the relaxation rates for each concentration were subsequently measured at the following frequencies: 870 MHz (20.4 T), 1050 MHz (24.7 T), 1200 MHz (28.2 T) and 1400 MHz (33 T). A specially designed single-resonance $^1$H-NMR probe was used enabling in situ tuning of the desired NMR frequencies. Data acquisition and data analysis were performed on a home-built variable-frequency NMR spectrometer covering Larmor frequency up to 2 GHz via a specially
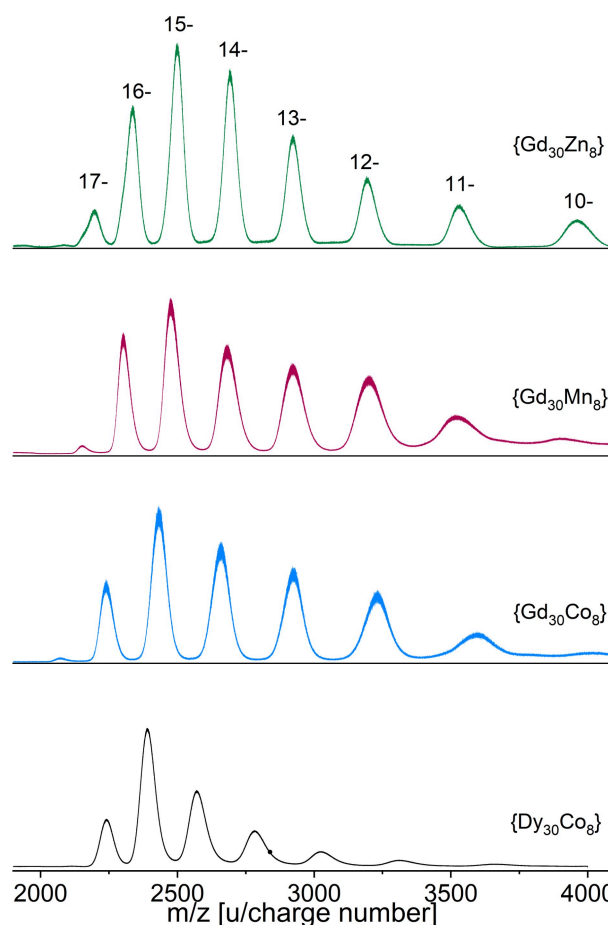


**Figure 6.** Negative ion HRESI-MS of the clusters showing different charge states of the intact clusters with varying number of counter cations and H$_2$O.

designed data acquisition and processing software. In order to cope with low field homogeneity of these magnets (axial second order gradient at the field's center of the order of 25 ppm/mm$^2$), small sample volumes (1 mm$^3$ in a 1 mm diameter capillary tube) were used, which were placed at the magnetic field center (better than 0.2–0.5 mm). Moreover, single scan experiments were used to minimize the impact of fast field fluctuations (up to 50 ppm) on the measurements. The experimental details are further described in ref. [20, 21, 24, 25, 33]. Temperature was recorded and found constant at 295 ± 2 K.

## $^1$H – Larmor Frequencies 20–400 MHz

The relaxation measurements at lower magnetic fields were measured on commercially available NMR instruments. The experimental details are described in ref. [20, 21, 24, 33] to which we refer here.

## Determination of the Relaxivities $r_1$ and $r_2$

Inversion recovery, progressive saturation recovery, and CPMG multi-echo pulse sequences were applied to measure $R_1$ and $R_2$. At each field and for the prepared series of cluster's concentrations between zero (pure solvent) and 1 mM, $R_1$ and $R_2$ were determined using mono-exponential fits to the data. In all cases no deviation of

the relaxation curves from a mono-exponential behavior was observed, which indicates that our solutions were homogenous during the NMR-measurements. Repeated measurements after months revealed the same relaxation curves. These findings allowed us to use the same samples for the complete range of magnetic fields, allowing for direct comparison of the relaxivities. During measurement and further data processing, $R_1$ and $R_2$ were plotted as a function of the cluster's concentration at each field. Evidence of the linear relation between concentration and relaxation rates was thus provided, as expected for PRE of a homogenous solution. The slope of the linear fit corresponds to the relaxivities $r_1$ and $r_2$. Please note that the cluster's concentration and not the single ion concentration is used. This is due to the fact that the observable PRE is caused by the complete cluster and cannot only be attributed to one single ion. Moreover, potential cooperative effects between the transition-metal ions (Co/Mn/Zn) and the lanthanides (Dy or Gd) need to be considered, which makes the ansatz of adding up the single ion contributions at least to be discussed.

## Conflict of Interest

The authors declare no conflict of interest.

## Data Availability Statement

The data that support the findings of this study are available from the corresponding author upon reasonable request.

[1] Q. L. Vuong, J. F. Berret, J. Fresnais, Y. Gossuin, O. Sandre, *Adv. Healthcare Mater.* **2012**, *1*, 502–512.

[2] Q. L. Vuong, S. Van Doorslaer, J. L. Bridot, C. Argante, G. Alejandro, R. Hermann, S. Disch, C. Mattea, S. Stapf, Y. Gossuin, *Magn. Reson. Mater Phy.* **2012**, *25*, 467–478.

[3] Y. Gossuin, A. Hocq, Q. L. Vuong, S. Disch, R. P. Hermann, P. Gillis, *Nanotechnology* **2008**, *19*.

[4] F. Carniato, L. Tei, M. Botta, E. Ravera, M. Fragai, G. Parigi, C. Luchinat, *ACS Appl. Bio Mater.* **2020**, *3*, 9065–9072.

[5] I. Bertini, C. Luchinat, G. Parigi, E. Ravera, *NMR of Paramagnetic Molecules - Applications to Metallobiomolecules and Models*, Elsevier, Amsterdam, **2017**.

[6] I. Bertini, C. Luchinat, G. Parigi, *Solution NMR of paramagnetic molecules: Applications to metallobiomolecules and models*, Elsevier Science B. V., Amsterdam, **2001**.

[7] I. Bertini, C. Luchinat, G. Parigi, *Adv. Inorg. Chem.* **2005**, *57*, 105–172.

[8] D. Kruk, J. Kowalewski, *J. Chem. Phys.* **2009**, *130*, 174104.

[9] E. Belorizky, P. H. Fries, L. Helm, J. Kowalewski, D. Kruk, R. R. Sharp, P. O. Westlund, *J. Chem. Phys.* **2008**, *128*, 052315.

[10] J. Svoboda, T. Nilsson, J. Kowalewski, P. O. Westlund, P. T. Larsson, *J. Magn. Reson. Ser. A.* **1996**, *121*, 108–113.

[11] L. Vander Elst, A. Roch, P. Gillis, S. Laurent, F. Botteman, J. W. M. Bulte, R. N. Muller, *Magn. Reson. Med.* **2002**, *47*, 1121–1130.

[12] I. Solomon, *Phys. Rev.* **1955**, *99*, 559–565.

[13] N. Bloembergen, L. O. Morgan, *J. Chem. Phys.* **1961**, *34*, 842–850.

[14] A. Abragam, *Principles of Nuclear Magnetism*, Oxford University Press, Oxford, **1961**.

[15] D. H. Powell, O. M. N. Dhubhghaill, D. Pubanz, L. Helm, Y. S. Lebedev, W. Schlaepfer, A. E. Merbach, *J. Am. Chem. Soc.* **1996**, *118*, 9333–9346.

[16] P. M. Singer, A. V. Parambathu, T. J. Pinheiro dos Santos, Y. Liu, L. B. Alemany, G. J. Hirasaki, W. G. Chapman, D. Asthagiri, *Phys. Chem. Chem. Phys.* **2021**, *23*, 20974–20984.

[17] A. M. Funk, P. Harvey, K. L. N. A. Finney, M. A. Fox, A. M. Kenwright, N. J. Rogers, P. K. Senanayake, D. Parker, *Phys. Chem. Chem. Phys.* **2015**, *17*, 16507–16511.

[18] M. Norek, J. A. Peters, *Prog. Nucl. Magn. Reson. Spectrosc.* **2011**, *59*, 64–82.

[19] M. Bottrill, L. K. Nicholas, N. J. Long, *Chem. Soc. Rev.* **2006**, *35*, 557–571.

[20] G. Guthausen, J. R. Machado, B. Luy, A. Baniodeh, A. K. Powell, S. Krämer, F. Ranzinger, M. P. Herrling, S. Lackner, H. Horn, *Dalton Trans.* **2015**, *44*, 5032–5040.

[21] J. R. Machado, A. Baniodeh, A. K. Powell, B. Luy, S. Krämer, G. Guthausen, *ChemPhysChem.* **2014**, *15*, 3608–3613.

[22] J. Elistratova, B. Akhmadeev, V. Korenev, M. Sokolov, I. Nizameev, I. Ismaev, M. Kadirov, A. Sapunova, A. Voloshina, R. Amirov, A. Mustafina, *J. Mol. Liq.* **2019**, *296*, 111821.

[23] S. Pizzanelli, R. Zairov, M. Sokolov, M. C. Mascherpa, B. Akhmadeev, A. Mustafina, L. Calucci, *J. Phys. Chem. C.* **2019**, *123*, 18095–18102.

[24] M. Ibrahim, S. Krämer, N. Schork, G. Guthausen, *Dalton Trans.* **2019**, *48*, 15597–15604.

[25] J. Kowalewski, P. H. Fries, D. Kruk, M. Odelius, A. V. Egorov, S. Krämer, H. Stork, M. Horvatić, C. Berthier, *J. Magn. Reson.* **2020**, *314*, 106737.

[26] M. Ibrahim, V. Mereacre, N. Leblanc, W. Wernsdorfer, C. E. Anson, A. K. Powell, *Angew. Chem. Int. Ed.* **2015**, *54*, 15574–15578; *Angew. Chem.* **2015**, *127*, 15795–15799.

[27] M. Ibrahim, Y. Peng, E. Moreno-Pineda, C. E. Anson, J. Schnack, A. K. Powell, *Small Structures* **2021**, *2*, 2100052.

[28] D. Cicolari, F. Santanni, L. Grassi, F. Brero, M. Filibian, T. Recca, P. Arosio, M. Perfetti, M. Mariani, R. Sessoli, A. Lascialfari, *J. Chem. Phys.* **2021**, *155*, 214201.

[29] I. Bertini, F. Briganti, Z. C. Xia, C. Luchinat, *J. Magn. Reson. Ser. A* **1993**, *101*, 198–201.

[30] F. J. Liu, S. Laurent, A. Roch, L. Vander Elst, R. N. Muller, *J. Nanomater.* **2013**.

[31] S. L. C. Pinho, S. Laurent, J. Rocha, A. Roch, M. H. Delville, S. Mornet, L. D. Carlos, L. Vander Elst, R. N. Muller, C. F. G. C. Geraldes, *J. Phys. Chem. C.* **2012**, *116*, 2285–2291.

[32] G. Pintacuda, M. John, X. C. Su, G. Otting, *Acc. Chem. Res.* **2007**, *40*, 206–212.

[33] A. C. Venu, R. Nasser Din, T. Rudszuck, P. Picchetti, P. Chakraborty, A. K. Powell, S. Krämer, G. Guthausen, M. Ibrahim, *Molecules.* **2021**, *26*, 7481.